Materials Science, Vol. 36, No. 3, 2000

DYNAMIC TENSION OF A CYLINDRICAL SPECIMEN WITH CIRCUMFERENTIAL CRACK

O. E. Andreikiv, V. M. Boiko, S. E. Kovchyk, and I. V. Khodan'

UDC 539.375: 620.186.4

We describe a method for the evaluation of the dynamic stress intensity factors under the action of dynamic loading. The method is based on the solution of the problem of limiting equilibrium for a cylindrical specimen of finite dimensions containing a circumferential crack. In the process of solution, we use the experimental load-time diagram. We establish a simple formula for the evaluation of the dynamic stress intensity factors depending on the history of loading of the specimen. The obtained results serve as a basis of an experimental procedure of determination of the crack-growth resistance of materials. The results of specially performed experimental investigations confirm the efficiency of the proposed formulas.

The analytic solutions of the problems of evaluation of the dynamic stress intensity factors (DSIF) for cracked bodies subjected to the action of impulsive loads can be constructed only for some simplified problems for infinite bodies. At the same time, the approximate solutions of applied problems are successfully constructed with the help of contemporary numerical methods and, in particular, the finite-element method. At the Karpenko Physicomechanical Institute of the Ukrainian Academy of Sciences, we developed a special software package capable of giving simple formulas for the numerical evaluation of the DSIF for finite cracked bodies subjected to the action of dynamic loads.

There are two basic procedures of experimental determination of the time dependence of the DSIF, namely, by using small-base sensors (as a disadvantage of this method, we can mention the necessity of pasting transducers to each specimen with subsequent calibration) or by the methods of photoelasticity or caustics. The application of the second method requires high-speed photography and, hence, advanced recording equipment. It is also characterized by a labor-consuming procedure of decoding the frames. Thus, its application seems to be reasonable only for reference measurements.

The theoretical methods for the evaluation of DSIF are, as a rule, base on the use of complicated models. These models describe only a part of dynamic effects and include experimentally measured characteristics. At present, the combined numerical and experimental approaches are used especially extensively. Thus, a procedure of processing the load–time diagrams for beam specimens subjected to one- and three-point impact bending was proposed in [1, 2]. In these works, the time dependence of the DSIF was studied with the help of the finite-element method and modal analysis [3, 4]. This approach to the solution of problems of dynamic fracture mechanics was originated by Nash [5] and developed in [1, 6]. It combines the availability of simplified models with the accuracy of the finite-element method. The methods and improvements close to this approach were proposed in [7–11].

If a cylindrical specimen containing an external circumferential crack is subjected to tension, then the local planar strained state is realized along the entire crack contour. This factor, together with high loading rates, imposes the severest possible restrictions, which makes its role determining (as compared with all other factors).

However, for cylindrical specimens, we do not know any investigations of the time dependence of the DSIF. Hence, we consider a cylindrical specimen of length $2h$ and radius a weakened in its middle with a surface circumferential crack of depth c (Fig. 1). Two equal forces $P(t)$ are applied to the end faces of the cylinder. Due to the symmetry of the problem, we consider only the upper half of the specimen. Since the problem is axially symmetric, the stresses are completely determined by two components of the displacements, i.e., the problem is, in fact, two-dimensional.

Prior to the initial time $t = 0$, the specimen was in the state of rest.

Karpenko Physicomechanical Institute, Ukrainian Academy of Sciences, L'viv. Translated from Fizyko-Khimichna Mekhanika Materialiv, Vol. 36, No. 3, pp. 59–66, May–June, 2000. Original article submitted September 15, 1999.

 1068–820X/00/3603–0382 $25.00

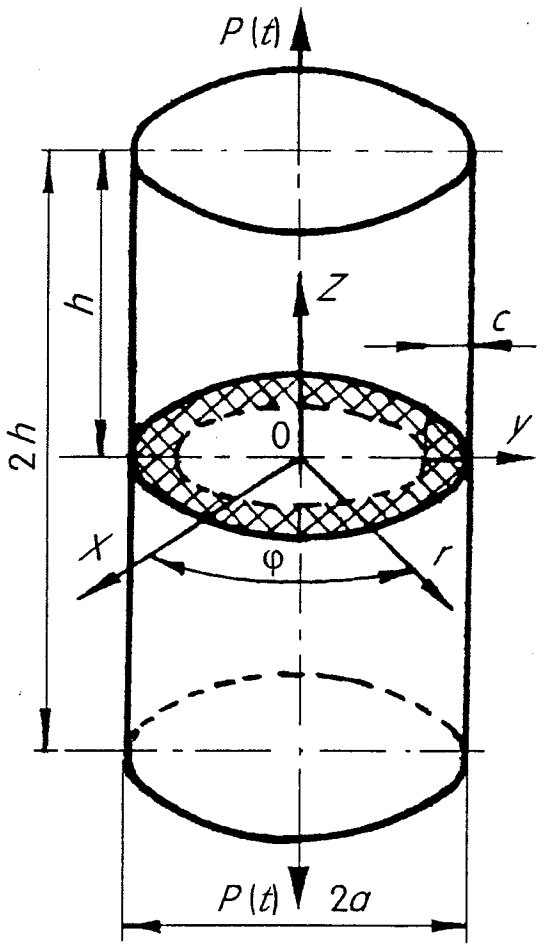

Fig. 1. Geometric parameters and the scheme of loading of a cylindrical specimen.

If a function $\Lambda(t)$ reflects the response of the specimen at an arbitrary point A with coordinates (r, z) to a unit pulse of a concentrated force applied at the point with coordinates $(0, h)$, then the normal displacement of the specimen $u(t)$ at the point A is described with the help of the Duhamel integral [12] as

$$u(t) = \int_0^t P(\tau)\Lambda(t-\tau)d\tau. \tag{1}$$

We approximate the function $P(t)$ by a broken line with N links, i.e.,

$$P(t) = \sum_{i=1}^{N} (k_i - k_{i-1})(t - t_{i-1})H(t - t_{i-1}), \tag{2}$$

where k_i are the angular coefficients of the links $(k_0 = 0)$, t_i are the abscissas of the salient points $(t_0 = 0)$, and $H(t)$ is the Heaviside function. Substituting expression (2) in relation (1), we obtain

$$u(t) = \sum_{i=1}^{N} (k_i - k_{i-1})\mathcal{R}(t - t_{i-1}), \tag{3}$$

where, according to (1),

$$\mathcal{R}(t_1) = H(t)\int_0^t \tau\Lambda(t-\tau)d\tau$$

is the normal displacement of the point A caused by a load applied to the end face of the cylinder and increasing with unit rate. One can find an expression similar to (3) for any linear system, by replacing the function $\Lambda(t)$ by the state-transition matrix of the corresponding boundary-value problem [12, 13]. Since the DSIF linearly depends on displacements near the crack tip, by analogy with (3), we obtain

$$K_I(t) = \sum_{i=1}^{N} (k_i - k_{i-1})K_I^{(1)}(t - t_{i-1}), \tag{4}$$

where $K_I^{(1)}(t)$ is the DSIF for the cylindrical specimen subjected to the action of the unit load $P(t) = 1 \times t$.

Further, we find $K_I^{(1)}(t)$ by the methods of modal analysis. The frequencies of natural vibrations ω_i and the corresponding displacements of the specimen (eigenvectors) are determined from the generalized eigenvalue problem [3, 4]

$$[J]\bar{\mathbf{u}} = \omega^2[M]\bar{\mathbf{u}} \tag{5}$$

with the following normalization conditions:

$$\mathbf{u}_i^t[M]\mathbf{u}_j = \delta_{ij}, \tag{6}$$

where $[K]$ is the stiffness matrix, $[M]$ is the matrix of masses [3], δ_{ij} is the Kronecker symbol, and the superscript "t" means that the matrix is transposed [4].

The component u_j of the vector of displacements can be expressed as follows [14]:

$$u_j(t) = \sum_{i=1}^{n} \frac{u_{Ii}u_{0i}}{\omega_i}\left[\int_0^t P(\tau)\sin\omega_i(t-\tau)d\tau\right], \tag{7}$$

where ω_i are the circular frequencies of natural vibrations of a half of the cylindrical specimen, n is the number of modes of natural vibrations taken into account in the analysis, and u_{ji} and u_{0i} are, respectively, the ith components of the vectors of displacements of the current point and the point of application of the force. Since the DSIF is proportional to the displacements on the crack surface, by analogy with (7), we can write

$$K_I(t) = \sum_{i=1}^{n} \frac{K_{Ii}u_{0i}}{\omega_i}\left[\int_0^t P(\tau)\sin\omega_i(t-\tau)d\tau\right],$$

where K_{Ii} is the stress intensify factor for the ith normalized mode of free vibrations of the cylinder. Substituting the load $P(t) = t$ in this expression, we get

$$K_I^{(1)}(t) = K_{IS}^{(1)}H(t)\left(t - \sum_{i=1}^{n}\left(\frac{\eta_i}{\omega_i}\right)\sin(\omega_i t)\right), \tag{8}$$

where $K_{IS}^{(1)}$ is the static stress intensify factor for the specimen stretched by the unit force applied to its end face (Fig. 1) and

$$\eta_i = \frac{K_{Ii} u_{0i}}{\omega^2 K_{IS}^{(1)}}.$$

By analogy with [1, 6], one can show that the equality

$$\sum_{i=1}^{n} \eta_i = 1 \tag{9}$$

serves as a criterion for the choice of n in Eq. (8). In view of relations (2) and (8), after simple transformations, we obtain

$$K_I(t) = K_{IS}^{(1)} P(t) - K_{IS}^{(1)} \sum_{i=1}^{N} (k_i - k_{i-1}) H(t - t_{i-1}) \sum_{i=1}^{n} \left(\frac{\eta_i}{\omega_i}\right) \sin \omega_j (t - t_{i-1}). \tag{10}$$

In relation (10), the DSIF is represented in the form of the sum of so-called quasistatic and inertial corrections. The dimensionless coefficients η_i and the natural frequencies

$$\omega_i^* = \frac{\omega_i a}{\sqrt{E/\rho}},$$

where E is Young's modulus and ρ is the density of the material, do not depend on the dimensions of the specimen. At the same time, they depend on the ratio of the length of the specimen to its radius, relative crack depth, and Poisson's ratio ν [4].

We determine the circular frequencies of natural vibrations and the corresponding eigenvectors by the method of Lanczos blocks [15] for the most interesting range of geometric parameters of the specimen: $0.3 \le \lambda \le 0.7$, $13.0 \le \gamma \le 20.0$ ($\lambda = c/a$ and $\gamma = 2h/a$), and $\nu = 0.3$. The results of numerical experiments carried out for different force–time loading diagrams and the analysis of relation (9) enable us to conclude that, within the indicated range of geometric parameters, for the evaluation of the DSIF, it suffices to consider five modes of free vibrations. We process the numerical data by the method of least squares and, as a result, arrive at the following polynomial approximations for ω_i^* and η_i:

$$\omega_1^* = 0.142 - 0.581\lambda + 0.629\lambda^2 + \frac{14.83\lambda - 22.32\lambda^2 + 6.417\lambda^3}{\gamma},$$

$$\omega_2^* = 0.393 - 1.511\lambda + 1.525\lambda^2 + \frac{44.48\lambda - 71.41\lambda^2 + 29.35\lambda^3}{\gamma},$$

$$\omega_3^* = 0.674 - 2.45\lambda + 2.347\lambda^2 + \frac{69.49\lambda - 109.28\lambda^2 + 47.67\lambda^3}{\gamma}, \tag{11}$$

$$\omega_4^* = 0.981 - 3.246\lambda + 3.034\lambda^2 + \frac{85.26\lambda - 127.75\lambda^2 + 53.8\lambda^3}{\gamma},$$

$$\omega_5^* = 1.191 - 3.117\lambda + 2.855\lambda^2 + \frac{90.77\lambda - 141.18\lambda^2 + 65.53\lambda^3}{\gamma},$$

$$\eta_1 = 1.228 + 0.358\lambda - 0.705\lambda^2 + (-0.0047\lambda + 0.0159\lambda^2)\gamma,$$

$$\eta_2 = -0.372 - 0.484\lambda + 1.133\lambda^2 + (0.0057\lambda - 0.0238\lambda^2)\gamma,$$

$$\eta_3 = 0.272 + 0.0755\lambda - 0.597\lambda^2 + (-0.0006\lambda + 0.0111\lambda^2)\gamma, \tag{12}$$

$$\eta_4 = -0.229 + 0.158\lambda + 0.19\lambda^2 - 0.0033\lambda\gamma,$$

$$\eta_5 = 0.14 - 0.337\lambda + 0.25\lambda^2 + (0.022\lambda - 0.03\lambda^2)\gamma.$$

The accuracy of approximation in relations (11) and (12) does not exceed 2.5 and 2%, respectively.

After this, we find the numerical values of ω_i^* and η_i for the range $0.27 \le \nu \le 0.33$. It was discovered that the values of ω_i^* and η_i are practically the equal for the first three modes. For the remaining modes, these parameters are slightly different [they are higher or lower than the values given by relations (11) and (12) by at most 0.003]. Taking into account the fact that the influence of these two modes on the DSIF is insignificant [this follows from the structure of relation (10) and the fact that the moduli of ω_i^* and η_i are small as compared with the corresponding values for the first three modes], we conclude that relations (11) and (12) can be applied within the range $0.27 \le \nu \le 0.33$ without serious loss of accuracy.

We also solved the eigenvalue problem (5), (6) for the following range of geometric parameters: $0.3 \le \lambda \le 0.7$ and $8.0 \le \gamma \le 13.0$. As follows from the results of the numerical experiments and the analysis of the coefficients η_i given by formula (9), for the evaluation of the DSIF according to relation (10), it suffices to consider three modes of free vibrations. For $\nu = 0.3$, we get the following polynomial approximations to ω_i^* and η_i:

$$\omega_1^* = -0.027 + 0.171\lambda - 0.064\lambda^2 + \frac{3.353 - 1.466\lambda - 1.806\lambda^2}{\gamma},$$

$$\omega_2^* = -0.0467 + 0.597\lambda - 0.596\lambda^2 + \frac{10.28 - 9.5942\lambda - 5.606\lambda^2}{\gamma}, \tag{13}$$

$$\omega_3^* = 0.138 + 0.594\lambda - 0.753\lambda^2 + \frac{13.795 - 10.92\lambda + 9.05\lambda^2}{\gamma},$$

$$\eta_1 = 1.242 + 0.313\lambda - 0.776\lambda^2 + (-0.0058\lambda + 0.0256\lambda^2)\gamma,$$

$$\eta_2 = -0.633 + 0.581\lambda + 0.215\lambda^2 + (0.0188 - 0.0708\lambda + 0.395\lambda^2)\gamma, \tag{14}$$

$$\eta_3 = 0.108 + 0.674\lambda - 1.117\lambda^2 + (0.0533\lambda - 0.188\lambda^2 + 0.176\lambda^3)\gamma.$$

In this case, the accuracy of approximation is not higher than 3 and 2.5%, respectively. As above, we determined the numerical values of the coefficients ω_i^* and η_i for the range $0.27 \le \nu \le 0.33$. Here, we can also use relations (13) and (14) without serious loss of accuracy. This follows from the fact that, for all three modes, the correlation of the coefficients ω_i^* and η_i does not exceed 2% in the most unfavorable cases.

Finally, we also studied the range $0.4 \le \lambda \le 0.8$ and $4.0 \le \gamma \le 8.0$. In this case, we observed the nonmonotonic convergence of the sum of the coefficients η_i to one for some small values of the parameter λ [see Eq. (9)]. A similar phenomenon was also discovered for plane beam specimens in [1, 4]. The results of numerical experi-

ments with different force–time loading diagrams and the analysis of relation (9) demonstrate that it suffices to consider two modes of free vibrations to guarantee the reliability of results. Clearly, this can be explained by the structure of relation (10) and the absolute values of ω_i^* and η_i for $i \geq 3$. For $\nu = 0.3$, by using the method of least squares, we obtain the following polynomial approximations:

$$\omega_1^* = -0.1013 + 0.6597\lambda - 0.51\lambda^2 + \frac{3.8903 - 5.0484\lambda + 1.4326\lambda^2}{\gamma},$$

$$\omega_2^* = 0.5576 - 0.7688\lambda + 0.3508\lambda^2 + \frac{5.7305 + 0.7167\lambda - 1.4534\lambda^2}{\gamma},$$

$$\eta_1 = 1.702 - 1.467\lambda + 0.773\lambda^2 + (-0.0528 + 0.197\lambda - 0.149\lambda^2)\gamma,$$

$$\eta_2 = -1.142 + 2.223\lambda - 1.082\lambda^2 + (0.069 - 0.224\lambda + 0.157\lambda^2)\gamma.$$

The accuracy of approximation in these formulas is equal to 2%. For η_2, it is equal to 4%.

Parallel with the coefficients ω_i^* and η_i, we computed the static stress intensity factor under the action of the unit force according to the scheme depicted in Fig. 1. It was shown that, within the analyzed ranges, this factor is practically independent of the length of the cylindrical specimen and Poisson's ratio ($0.27 \leq \nu \leq 0.33$). The error of its evaluation did not exceed 0.2% for $0.3 \leq \lambda \leq 0.8$. As a result, by the method of least squares, we obtained the following formula for the static stress intensity factor under the action of the unit force:

$$K_1 = \frac{Y(\lambda)}{r\sqrt{r}}, \tag{15}$$

where

$$Y(\lambda) = 3.403 - 29.637\lambda + 104.613\lambda^2 - 156.12\lambda^3 + 89.14\lambda^4. \tag{16}$$

There are several formulas for the function $Y(\lambda)$ available from the literature. Thus, in [16], it is represented in the form

$$Y(\lambda) = \sqrt{1-\varepsilon}\,\frac{1 - 0.5\varepsilon - 0.125\varepsilon^2 + 0.2757\varepsilon^3 - 0.2082\varepsilon^4 + 0.0663\varepsilon^5 + 0.0048\varepsilon^6 - 0.013\varepsilon^7}{2\varepsilon\sqrt{\varepsilon}}. \tag{17}$$

Here and in what follows, $\varepsilon = 1 - \lambda$. In [17], this function is given by the formula

$$Y(\lambda) = \sqrt{\lambda}\,\frac{1 + 0.5\varepsilon + 0.375\varepsilon^2 - 0.363\varepsilon^3 + 0.731\varepsilon^4}{2\varepsilon\sqrt{\pi\varepsilon}}. \tag{18}$$

These formulas were deduced by the method of limiting interpolation. The numerical values of this function obtained by the method of integral equations can be found in [18].

The data obtained according to these formulas are in fairly good agreement (Fig. 2) but the best correlation is observed between relation (16) and the numerical data from [18]. In our opinion, relation (16) guarantees the maximum possible accuracy of results for $0.3 \leq \lambda \leq 0.8$.

By using the equations presented above, we found the DSIF for the cylindrical steel specimen loaded according to the scheme depicted in Fig. 1. The specimen was 16 mm in diameter and 120 mm in length. The diameter of the neck was equal to 8.2 mm.

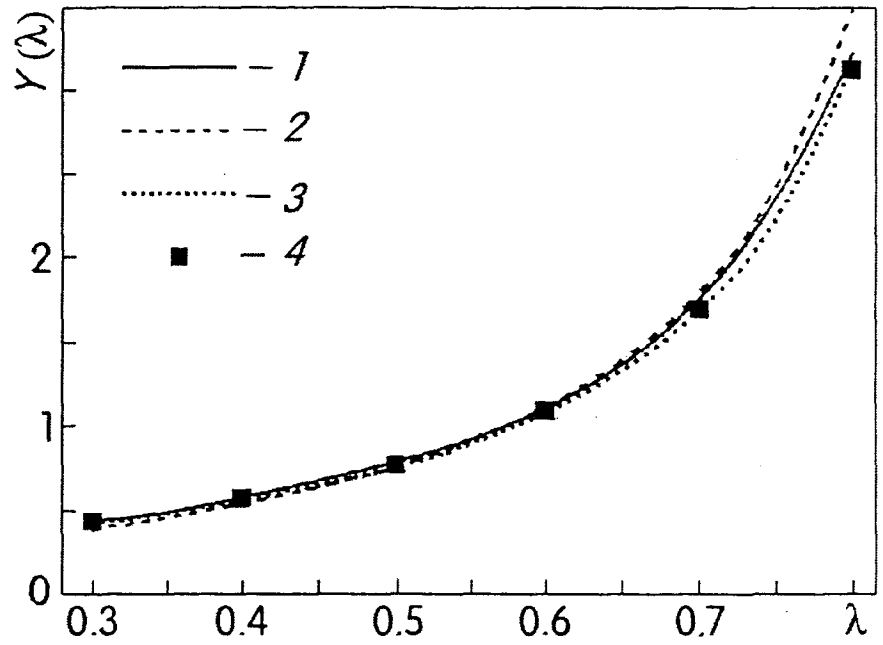

Fig. 2. Values of the function $Y(\lambda)$ obtained by different methods: (1) Eq.(16), (2) Eq.(17), (3) Eq.(18), (4) numerical data from [18].

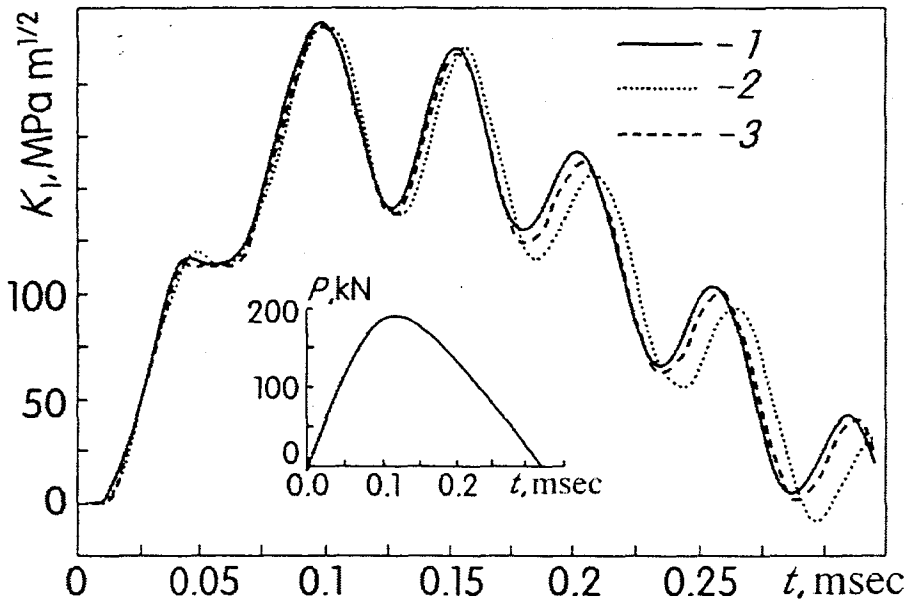

Fig. 3. Comparison of the values of DSIF obtained according to relation (10) and by the finite-element method: (1) relation (10), (2) finite-element method, $\Delta t = 5\,\mu$sec, (3) finite-element method, $\Delta t = 1\,\mu$sec.

We took the following elastic characteristics: $E = 200$ GPa, $\rho = 7.87$ Mg/m^3, and $\nu = 0.3$. In the force–time loading diagram (Fig. 3), the DSIF are presented as functions of time. To check the reliability of the results obtained according to formulas (10)–(12) and (16), we analyzed the time dependence of the DSIF by using the finite-element method together with the Newmark method [4] for two time steps $\Delta t = 1\,\mu$sec and $\Delta t = 5\,\mu$sec. The values of DSIF obtained according to formula (10) and with the help of the finite-element method for $\Delta t = 1\,\mu$sec are in very good agreement (Fig. 3).

To find the DSIF, one can also use the approach proposed in [19] and checked for the case of one- and three-point bending of a beam specimen [7, 20].

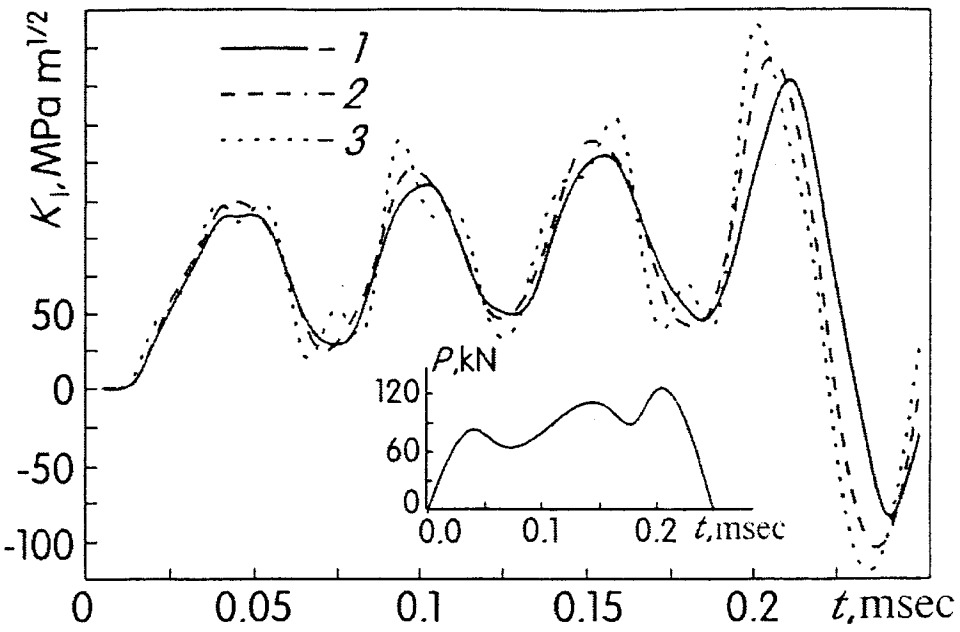

Fig. 4. Comparison of the DSIF obtained by using: (1) relation (10), (2) relation (19) with $m = 15$, (3)) relation (19) with $m = 10$.

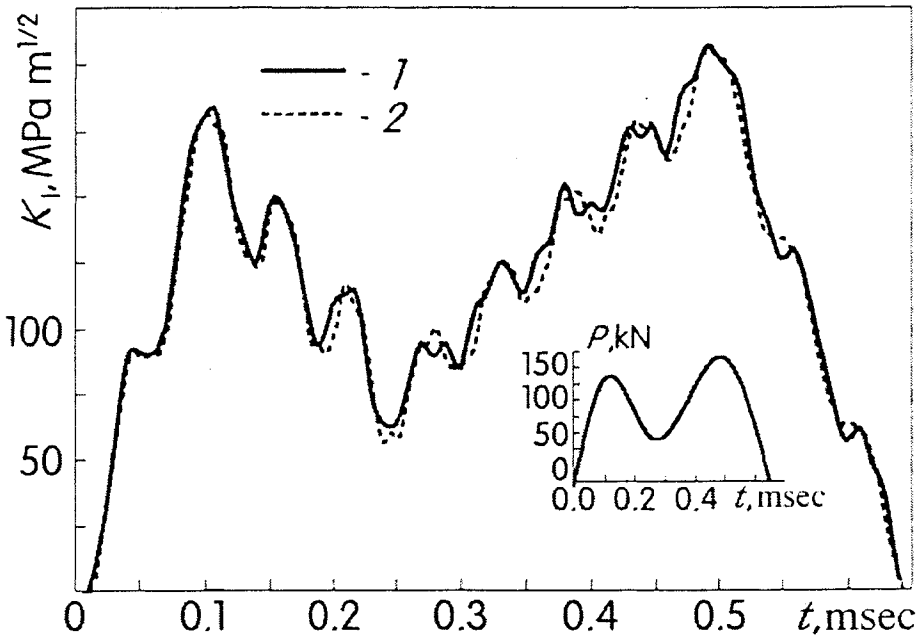

Fig. 5. Dependences of the DSIF on the loading history of the specimen of AK-42 steel (force–time loading diagram on the bases of the impact-testing machine): (1) relation (10), (2) finite-element method, $\Delta t = 1\ \mu$sec.

For this purpose, in the time interval $[0, T]$, we represent the load $P(t)$ in the form of its Fourier series:

$$P(t) \approx \frac{a_0}{2} + \sum_{k=0}^{m} (a_k \cos kpt + b_k \sin kpt), \qquad p = \frac{2\pi}{T}.$$

After simple transformations (for details, see [20]), we obtain the following expression for the DSIF in the cylindrical specimen stretched by two concentrated forces

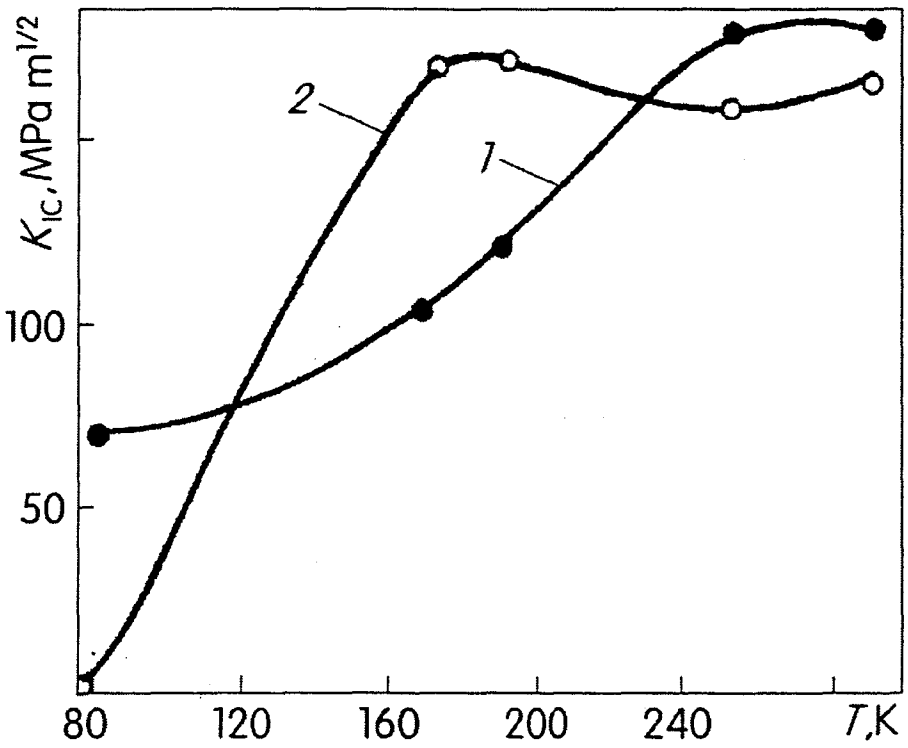

Fig. 6. Temperature dependences of the stress intensity factors for specimens of AK-42 steel under dynamic (1) and static (2) loading.

$$K_I(t) = K_{IS}^{(1)} \sum_{i=1}^{m} \eta_i \{A_i \sin \omega_i t + B_i \cos \omega_i t\} + \frac{a_0}{2} + \sum_{k=1}^{m} \frac{1}{1-(kp/\omega_i)^2} (a_k \cos kpt + b_k \sin kpt), \qquad (19)$$

where

$$A_i = -\frac{p}{\omega_i} \sum_{k=1}^{m} \frac{k b_k}{1-(kp/\omega_i)^2} \quad \text{and} \quad B_i = -\frac{a_0}{2} - \sum_{k=1}^{m} \frac{a_k}{1-(kp/\omega_i)^2}.$$

To check formula (19), we studied a steel specimen 120 mm in length and 16 mm in diameter. The diameter of the neck was equal to 9.4 mm. The results obtained by using relations (10) and (19) with $m = 15$ are well correlated (Fig. 4). This confirms the conclusion that the accuracy of the results given by relation (19) is satisfactory if we take $m = 10$–15 (see [19]). A criterion for the estimation of m can also be found in [8].

In our opinion, relation (10) is more convenient for the evaluation of the DSIF according to the force–time loading diagram. Indeed, if we use relation (19), then it is necessary to perform a cumbersome procedure of determination of the coefficients of the Fourier expansion of the loading function.

To develop the experimental aspects of the proposed method of finding K_I^D, we compared the results obtained by using the load–time diagrams recorded on the bases and on the hammer of an impact-testing machine. This procedure and the corresponding equipment were described in [21]. We tested specimens of AK-42 pressure-vessel steel. For various reasons [4], the diagrams recorded on the hammer of the impact-testing machine are more convenient and better reflect the actual processes. There are no significant discrepancies between the maximum values of K_I^D obtained on the bases and on the hammer (Figs. 3 and 5). Indeed, the indicated discrepancies vary within the range 5–8% for a large series of experiments carried out within at temperatures of 77–293°K. However, the periods of time covered by the diagrams recorded on the hammer are shorter than for the diagrams recorded on the bases for almost all specimens. Probably, this better corresponds to the character of fracture of the specimen. By using these diagrams, we plotted the curves of cold brittleness (Fig. 6) according to the proposed procedure (curve 1) and

under static loading (curve 2). As in the major part of works available from the literature (see, e.g., [22]), the threshold of cold brittleness in the dynamic tests is shifted to the right (toward higher temperatures).

The proposed method enables one to determine the time dependences of the DSIF with sufficiently high accuracy and can be regarded as a new step in the development of numerical-experimental approaches to the evaluation of the dynamic characteristics of structural materials.

REFERENCES

1. O. E. Andreikiv and I. V. Rokach, "A simplified method for the determination of the time dependence of the stress intensity factor in testing beam specimens for support-free impact bending," *Fiz.-Khim. Mekh. Mater.*, **25**, No. 5, 42–51 (1989).
2. I. V. Rokach, "A simplified method for the determination of the time dependence of the dynamic stress intensity factor in testing beam specimens for three-point impact bending," *Fiz.-Khim. Mekh. Mater.*, **26**, No. 3, 79–83 (1990).
3. O. C. Zienkiewich, *The Finite Element Method in Engineering Science*, McGraw-Hill, London (1971).
4. V. Z. Parton and V. G. Boriskovskii, *Dynamic Fracture Mechanics* [in Russian], Mashinostroenie, Moscow (1985).
5. G. E. Nash, "An analysis of the forces and bending moments generated during the notched beam impact test," *Eng. Fract. Mech.*, **5**, 269–285 (1969).
6. V. G. Boriskovskii and V. Z. Parton, "Numerical analysis of the intensity factors in a square plate with central crack under vibration loading by the finite-element method," in: *Improvement of the Design of Machines and Equipment in Chemical Industry* [in Russian], Izd. MIKhM, Moscow (1982), pp. 20–22.
7. I. V. Rokach, "Modal approach for processing one- and three-point bend test data for DSIF-time diagram determination. Part 1. Theory," *Fatigue Fract. Eng. Mat. Struct.*, **21**, 1007–1014 (1998).
8. I. V. Rokach, "Modal approach for processing one- and three-point bend test data for DSIF-time diagram determination. Part 2. Calculations and results," *Fatigue Fract. Eng. Mat. Struct.*, **21**, 1015–1026 (1998).
9. K. Kishimoto, S. Aoki, and M. Sakata, "Simple formula for dynamic stress intensity factors of precracked Charpy specimen," *Eng. Fract. Mech.*, **13**, 501–508 (1980).
10. K. Kishimoto, K. Kuroda, S. Aoki, and M. Sakata, "Simple formulae for dynamic fracture mechanics parameters of elastic and viscoelastic three-point bend specimens based on Timoshenko's beam theory," in: *Proc. of the Sixth Internat. Conf. on Fracture*, Vol. 5, Pergamon, Oxford (1984), pp. 3177–3184.
11. K. Kishimoto, K. Fujino, S. Aoki, and M. Sakata, "A simple formula for the dynamic stress intensity factor of a freely-supported bend specimen," *JSME Int. J., Ser. I*, **33**, 51–56 (1990).
12. V. G. Biderman, *Theory of Mechanical Vibrations* [in Russian], Vysshaya Shkola, Moscow (1980).
13. G. A. Korn and T. M. Korn, *Mathematical Handbook for Scientists and Engineers. Definitions, Theorems, and Formulas for Reference and Review*, McGraw-Hill, New York (1968).
14. S. Timoshenko, D. H. Young, and W. Weaver, Jr., *Vibration Problems in Engineering*, Wiley, New York (1974).
15. R. G. Grimes, J. G. Lewis, and H. D. Simon, "A shield block Lanczos algorithm for solving sparse symmetric generalized eigenproblems," *SIAM J. Matrix Anal. Appl.*, **15**, No. 1, 228–272 (1994).
16. V. V. Panasyuk, O. E. Andreikiv, and S. E. Kovchyk, *Methods for the Evaluation of Crack Resistance of Structural Materials* [in Russian], Naukova Dumka, Kiev (1977).
17. J. P. Benthem and W. T. Koiter, "Asymptotic approximations to crack problems," in: *Methods of Analysis and Solutions of Crack Problems*, Nordhoff, Leyden (1973), pp. 131–178.
18. L. M. Keer, J. M. Freedman, and H. A. Watts, "Infinite tensile cylinder with circumferential edge crack," *Lett. Appl. Eng. Sci.*, **5**, 129–139 (1977).
19. G. Wich, *Ein Beitrag zur Ermittlung von Risszähigkeiten bei schlagartiger Belastung*, PhD Thesis, München (1986).
20. O. E. Andreikiv, S. E. Kovchyk, I. V. Khodan', and V. M. Boiko, "On the methods for the evaluation of the dynamic crack-growth resistance of structural materials," *Probl. Mashinostr. Avtomat.*, No. 5–6, 22–35 (1997).
21. S. E. Kovchyk, I. V. Khodan', T. S. Zamora et al., "Information and measuring system for the dynamic investigation of structural materials," *Fiz.-Khim. Mekh. Mater.*, **30**, No. 3, 133–136 (1994).
22. I. V. Khodan', S. E. Kovchyk, and V. M. Boiko, "Development and verification of new experimental procedures aimed at the prediction of the behavior of structural materials under dynamic loading," in: *Mechanics and Physics of Fracture of Building Materials and Structures* [in Ukrainian], Kamenyar, L'viv (1998), pp. 561–567.